Chinese Chemical Letters 33 (2022) 4121–4125

Contents lists available at ScienceDirect

Chinese Chemical Letters

journal homepage: www.elsevier.com/locate/cclet

Hyperbenzones A and B, two 1,2-*seco* and rearranged polycyclic polyprenylated acylphloroglucinols from *Hypericum beanii*

Weijia Lu, Yanqiu Zhang, Yawei Li, Shengtao Ye, Jun Luo, Lingyi Kong*, Wenjun Xu*

Jiangsu Key Laboratory of Bioactive Natural Product Research and State Key Laboratory of Natural Medicines, School of Traditional Chinese Pharmacy, China Pharmaceutical University, Nanjing 210009, China

ARTICLE INFO

Article history:
Received 9 September 2021
Revised 17 October 2021
Accepted 4 November 2021
Available online 10 November 2021

Keywords:
seco-PPAPs
Hypericum beanii
Hyperbenzones A and B
NASH
1,2-*seco*-Bicyclic derivatives

ABSTRACT

Two novel *seco*-polycyclic polyprenylated acylphloroglucinols (PPAPs), hyperbenzones A (**1**) and B (**2**), were isolated from the roots of *Hypericum beanii*, together with one known biosynthetic congener **3**. Compound **1** incorporates a 6/5/5 ring system with an unprecedented spiro[bicyclo[3.3.0]octane-3,1′-cyclohexane]-2,2′–dione motif. The structures of **1** and **2** were determined by a combination of high resolution electrospray ionization mass spectroscopy (HRESIMS), nuclear magnetic resonance (NMR) spectroscopic analyses, gage-independent atomic orbital (GIAO) NMR chemical shift calculation with DP4+ analyses, electronic circular dichroism (ECD) calculation, and X-ray diffraction analysis. A 1,2-*seco* retro-Claisen rearrangement from a bicyclo[3.3.1]nonane PPAP precursor and following chemodivergent radical cascade cyclizations are proposed as the key steps in the biosynthetic pathway to yield compounds **1** and **2**. Biological investigations indicated that compounds **1** and **3** could decrease intracellular lipid accumulation in a palmitic acid-induced nonalcoholic steatohepatitis (NASH) cell model.

Polycyclic polyprenylated acylphloroglucinols (PPAPs), most of which feature highly oxygenated and densely substituted bicyclo[3.3.1]nonane-2,4,9-trione core, have become one of the hotspots in the natural products research field [1–3]. The enolizable β-diketones and β,β'-triketones in the core are versatile units to undergo ring-opening and further rearrangement reactions, which have strikingly expanded the structural complexity and diversity of PPAPs [4,5]. Up to date, 40 bicyclo[3.3.1]nonane-derived *seco*-PPAPs, including 1,2-*seco*, 2,3-*seco*, 3,4-*seco*, 1,9-*seco*, 1,2;4,5-*diseco*, and their highly cyclized derivatives with intriguing architectures, have been reported [2,6-10]. It is noting that *seco*-PPAPs exhibit a wide range of biological activities, including anti-inflammatory [8], anti-tumor [9,10], acetylcholinesterase (AChE) inhibitory activities [11], and multidrug resistance reversal activity to adriamycin resistant cancer cell lines [12].

In our continuous high-performance liquid chromatography-diode array detection (HPLC-DAD) and proton nuclear magnetic resonance (^{1}H NMR) guided pursuit of benzoyl-PPAPs from *Hypericum beanii* (*H. beanii*) [13,14], hyperbenzones A (**1**) and B (**2**), together with one known biosynthetic congener otogirinin D (**3**) [15] were isolated (Fig. 1 and Scheme 1). Notably, hyperbenzone A (**1**) is the first example of 1,2-*seco*-PPAP with an unprecedented spiro[bicyclo[3.3.0]octane-3,1′-cyclohexane]-2,2′–dione motif, while hyperbenzone B (**2**) possess an unusual 4,4-dimethyl-3-oxabicyclo[3.1.0]hexan-2-one moiety. Compounds **1** and **2** could biogenetically arise from an assumed bicyclo[3.3.1]nonane PPAP precursor *via* 1,2-*seco* retro-Claisen rearrangement and chemodivergent radical cascade cyclizations. Determination of the planar structures of **1** and **2** based on high resolution electrospray ionization mass spectroscopy (HRESIMS) and two-dimensional nuclear magnetic resonance (2D NMR) experiments, while the estab-

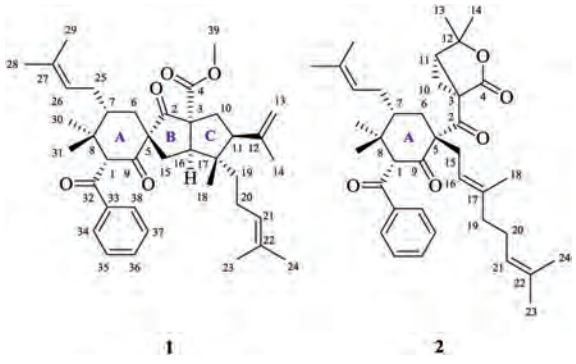

Fig. 1. Structures of hyperbenzones A (**1**) and B (**2**).

* Corresponding authors.
E-mail addresses: wjxu@cpu.edu.cn (W. Xu), cpu_lykong@126.com (L. Kong).

https://doi.org/10.1016/j.cclet.2021.11.011
1001-8417/

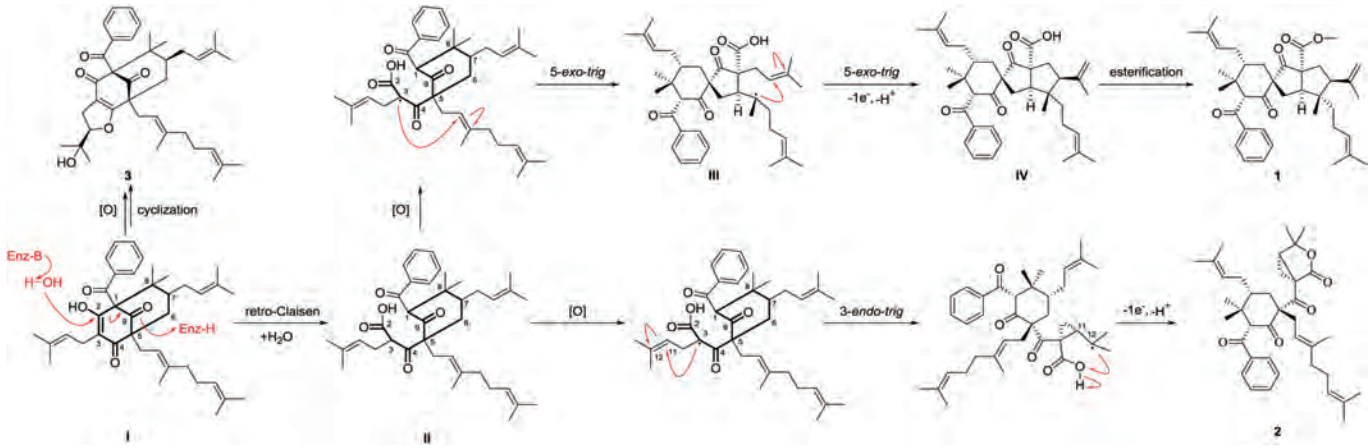

Scheme 1. Putative biosynthetic pathway for compounds **1**–**3**.

lishment of their absolute configurations was confirmed by X-ray diffraction analysis, and gage-independent atomic orbital (GIAO) NMR chemical shift calculations with DP4+ analyses, and comparison of the experimental and calculated electronic circular dichroism (ECD) data. Detailed herein are the isolation, structural elucidation, and the plausible biosynthetic pathway of compounds **1**–**3** along with their *in vitro* effects against nonalcoholic steatohepatitis (NASH).

Hyperbenzone A (**1**) was isolated as a white powder and eventually as colorless needle crystals from MeOH–H_2O (90:10) system. The molecular formula was assigned from the HRESIMS protonated molecular ion at *m/z* 601.3877 $[M+H]^+$ (calcd. 601.3888) as $C_{39}H_{52}O_5$, which indicated 14 indices of hydrogen deficiency. The ^1H NMR spectrum (Table 1) showed obvious signals of five aromatic protons (δ_H 7.79, 2H, br d, $J=7.2$ Hz; 7.55, 1H, br t, $J=7.4$ Hz; and 7.46, 2H, br dd, $J=7.4$, 7.2 Hz), four olefinic protons (δ_H 5.13, t, $J=6.9$ Hz; 5.09, t, $J=7.2$ Hz; 4.90, br s; and 4.68, br s), and nine methyls (δ_H 3.53, s; 1.72, s, overlapped; 1.72, s, overlapped; 1.71, s; 1.64, s; 1.61, s; 1.17, s; 1.11, s; and 0.63, s). The ^{13}C NMR (Table 1) and distortionless enhancement by polarization transfer (DEPT) spectra, in conjunction with a heteronuclear single quantum coherence (HSQC) experiment, indicated characteristic resonances of two non-conjugated carbonyl groups (δ_C 210.5 and 206.3), a benzoyl group (δ_C 196.0, 139.0, 133.1, 128.8 × 2, and 127.8 × 2), an ester carbonyl group (δ_C 170.2), two trisubstituted olefine (δ_C 133.8, 131.9, 124.5, and 122.8), and one terminal double bond (δ_C 142.9 and 113.9). These functionalities accounted 11 out of 14 indices of hydrogen deficiency, and the remaining three ones were attributable to the existence of a tricyclic ring system in **1**.

Two-dimensional NMR spectra analysis allowed the assembly of units a and b and their connectivity in **1** (Fig. 2). The correlations from the *gem*–dimethyl groups Me-30 and Me-31 to C-1, C-7 and C-8, from H_2-6 to C-5, C-7 and C-9, and from H-1 to C-7, C-8 and C-9 in the heteronuclear multiple bond correlation (HMBC) spectrum, as well as ^1H–^1H correlation spectroscopy (COSY) cross-peak of H_2-6/H-7 established a cyclohexanone ring A in unit a. The locations of the benzoyl and an isoprenyl group at C-1 and C-7, respectively, were assigned by the HMBC correlations from H-1 to C-32, and from H_2-25 to C-6, C-7, C-8 and C-26. Thus, unit a with a cyclohexanone ring A was defined as shown in Fig. 2.

The HMBC correlations from H_2-15 to C-2, C-5, C-16 and C-17, from H-16 to C-2, C-3, C-5, C-10, C-11, C-15 and C-17, and from H-11 to C-3, C-10, C-16 and C-17 as well as the spin systems of H_2-10/H-11, and H_2–15/H-16 indicated the presence of a hexahydropentalen-1(2*H*)-one moiety (rings B and C) in unit b. The correlations from H_2-10 and H-16 to C-4, from Me-39 to C-4, from

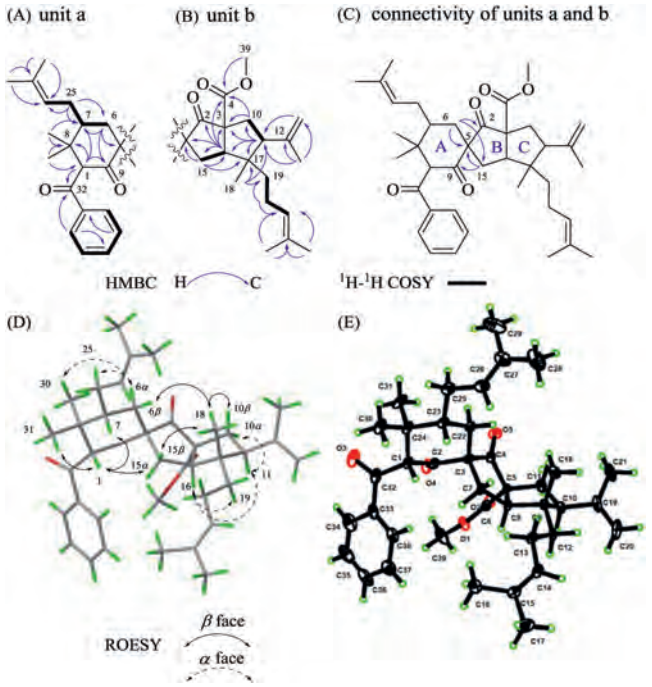

Fig. 2. Two-dimensional NMR spectra analysis and crystallographic analysis of **1**. (A–D) Key HMBC, ^1H–^1H COSY, and ROESY correlations of **1**. (E) The X-ray Oak Ridge thermal ellipsoid plot (ORTEP) drawing of **1**.

Me-14 and H_2-13 to C-11, from Me-18 and H_2-19 to C-11, C-16, and C-17, and from H_2-20 to C-19 and C-21 in the HMBC spectrum indicated the locations of a methyl ester, an isopropenyl, a methyl, and a homoprenyl group in unit b. Finally, the diagnostic-HMBC correlations from H_2-6 to C-2, C-5, and C-15, and from H_2-15 to C-5 and C-9 disclosed the connectivity of units a and b *via* a C-5 spirocenter. Thus, an unprecedented spiro[bicyclo[3.3.0]octane-3,1′-cyclohexane]-2,2′–dione scaffold in **1** was identified as depicted (Fig. 2).

The relative configuration of hyperbenzone A (**1**) was determined using a rotating-frame Overhauser effect spectroscopy (ROESY) experiment, in which correlations of H-1/H-7, H-1/Me-31, H-6α/Me-30, and H-6α/H-25b supported that H-1 and H-7 in unit a are β-oriented (Fig. 2D). The ROESY cross-peaks of H-1/H-7, H-10α/H-11, Me-18/H-10β, and Me-18/H-15β indicated the α-orientations of H-11 and H-16, and the β-orientation of Me-18

Table 1
^{1}H (600 MHz) and ^{13}C (150 MHz) NMR data of **1**[a] and **2**[a].

No.	Hyperbenzone A (**1**)		Hyperbenzone B (**2**)	
	δ_H (J in Hz)	δ_C	δ_H (J in Hz)	δ_C
1	4.57, s	63.9	4.73, s	64.0
2		210.5		201.6
3		66.8		39.7
4		170.2		171.4
5		66.0		66.2
6α	2.15, br dd (14.3, 13.6)[b]	35.7	2.11, br dd (14.0, 12.4)	34.6
6β	1.75, dd (14.3, 3.2)[b]		2.00, dd (14.0, 3.6)[b]	
7	1.68, m[b]	46.1	1.81, m[b]	44.8
8		44.4		45.9
9		206.3		206.3
10	α 2.25, dd (13.6, 6.7)[b]	36.4	a 1.89, dd (11.4, 7.9)	25.1
	β 2.19, dd (13.6, 13.2)[b]		b 1.45, br dd (11.4, 10.9)	
11	2.40, dd (13.2, 6.7)	56.1	2.60, dd (10.9, 7.9)	40.1[b]
12		142.9		80.9
13	a 4.90, br s	113.9	1.49, s	28.6
	b 4.68, br s			
14	1.72, s[b]	24.0	1.31, s	24.4
15	α 2.62, dd (14.4, 10.0)	34.3	a 3.42, dd (15.1, 6.1)	30.8
	β 1.99, dd (14.4, 5.3)[b]		b 3.06, dd (15.1, 7.9)	
16	3.18, dd (10.0, 5.3)	49.3	4.78, br dd (7.9, 6.1)	117.2
17		47.0		140.1
18	0.63, s	17.1	1.72, s	17.0
19a	1.50, td (12.9, 12.2, 4.9)	42.1	1.96, m[b]	40.1[b]
19b	1.40, td (13.5, 13.0, 5.0)		1.96, m[b]	
20a	2.11, m[b]	23.98	2.00, m[b]	26.6
20b	2.00, m[b]		1.97, m[b]	
21	5.13, t (6.9)	124.5	5.01, t (6.0)	123.8
22		131.9		131.9
23	1.72, s[b]	26.0	1.66, s	25.8
24	1.64, s	18.2	1.57, s	17.8
25a	2.26, m[b]	27.2	2.26, m[b]	27.6
25b	1.79, m[b]		1.79, m[b]	
26	5.09, t (7.2)	122.8	5.09, m	123.1
27		133.8		133.4
28	1.71, s[b]	25.9	1.70, s	26.0
29	1.61, s	17.9	1.62, s	18.1
30	1.17, s	16.1	1.23, s	16.0
31	1.11, s	27.0	1.16, s	27.8
32		196.0		196.0
33		139.0		138.9
34, 38	7.79, br d (7.2)[b]	127.8[b]	7.91, br d (7.5)[b]	128.2[b]
35, 37	7.46, br dd (7.4, 7.2)[b]	128.8[b]	7.45, br dd (7.5, 7.4)[b]	128.7[b]
36	7.55, br t (7.4)	133.1	7.52, br t (7.4)	132.9
39	3.53, s	53.3		

[a] Measured in $CDCl_3$.
[b] Overlapped signals.

(unit b). In addition, the key ROESY correlations of H-1/H-15α, and Me-18/H-6β indicated that the C-15 to C-17 hemi-sphere in unit b is located at the upside of the C-5 spirocenter (Fig. 2D). However, due to the absence of obvious ROESY correlations between Me-39 with other protons, the relative configuration of C-3 was still indistinct. To tackle this problem, we carried out computational modeling of NMR chemical shifts of two possible C-3 epimers, named (3*R**)-**1a** and (3*S**)-**1b**. The absolute difference between calculated and experimental ^{13}C NMR chemical shifts of (3*R**)-**1a** were within 5 ppm, while the calculated ^{13}C NMR chemical shifts of (3*S**)-**1b** showed large discrepancies at C-1, C-5, C-10, C-12, C-16, C-17, C-33, and C-37 (Fig. 3A). Further, the DP4+ NMR chemical shift calculation method confirmed the assignment of an *R** configuration for C-3 (Fig. 3B and Fig. S1-1A in Supporting information). Thus, the C-3 methyl ester group in **1** was assigned as α-orientation (3*R**). Then, we tried many recipes to obtain a suitable single crystal for X-Ray diffraction analysis, but only got a thin needle crystal for Mo Kα radiation analysis. And the relative configuration of **1** was thus confirmed by the subsequent crystallographic analysis (Fig. 2E) [CCDC 2091426], which is also consistent with that of (3*R**)-**1a**. On the basis of this well-defined relative configuration of **1**, the absolute configuration of **1** was confirmed as 1*S*,3*R*,5*R*,7*R*,11*S*,16*R*,17*S* by ECD theoretical calculations (Fig. 3C).

Hyperbenzone B (**2**) was purified as a yellow oil. The molecular formula of **2** was determined as $C_{38}H_{50}O_5$ on the basis of its HRESIMS and ^{13}C NMR data (Table 1) and indicated 14 indices of hydrogen deficiency. Comparison of its 1D (Table 1) and 2D NMR spectroscopy data with those of **1** indicated that **2** had the same benzoyl group and cyclohexanone ring A. A comprehensive analysis of DEPT and HSQC spectra suggested that C-3 (δ_C 39.7) is a quaternary carbon, C-11 (δ_C 40.1, overlapped) is a tertiary carbon, and C-19 is a secondary carbon (δ_C 40.1, overlapped). The prominent HMBC correlations from H-10a to C-3, from H-10b to C-11, and from H-11 to C-3 and C-10, as well as ^{1}H–^{1}H COSY cross-peaks of H_2-10/H-11 established a cyclopropane ring in compound **2**. And the HMBC correlations from to H_2-10 to C-4 and C-12, from H-11 to C-4 and C-12, and from *gem*–dimethyl groups Me-13 and Me-14 to C-11 and C-12 indicated the presence of a 4,4-dimethyl-3-oxabicyclo[3.1.0]hexan-2-one moiety in compound **2** (Fig. 4A), which is similar to that in a known compound hypercohin K [16]. In addition, a geranyl group was deduced by the HMBC correlations from allylic Me-18 to C-16, C-17 and C-19, from H-21

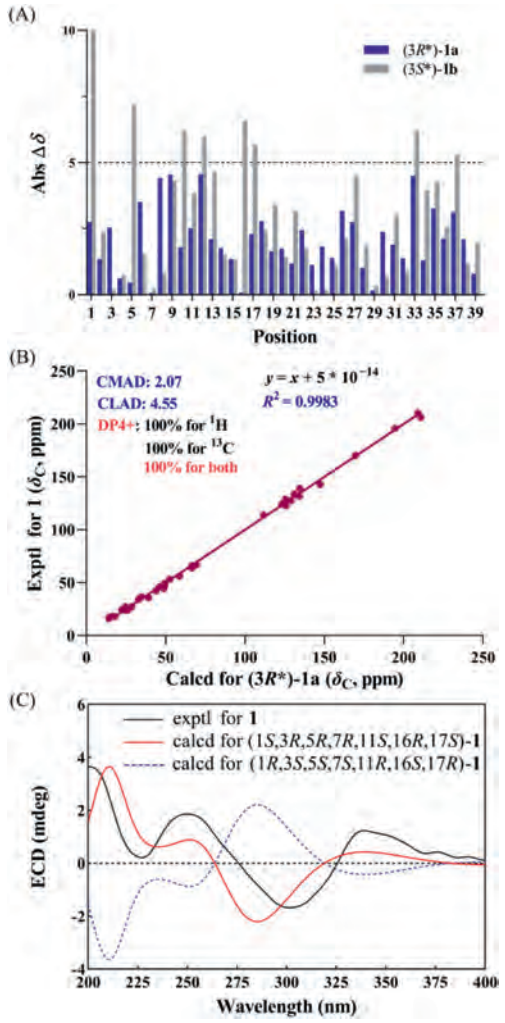

Fig. 3. A comprehensive methodology for determination of relative and absolute configurations of compound **1**: (A) Absolute difference between calculated and experimental ^{13}C NMR chemical shifts of (3R*)-**1a** and (3S*)-**1b**. (B) NMR calculations with DP4+ analyses for (3R*)-**1a**. (C) Experimental and calculated ECD spectra of **1**.

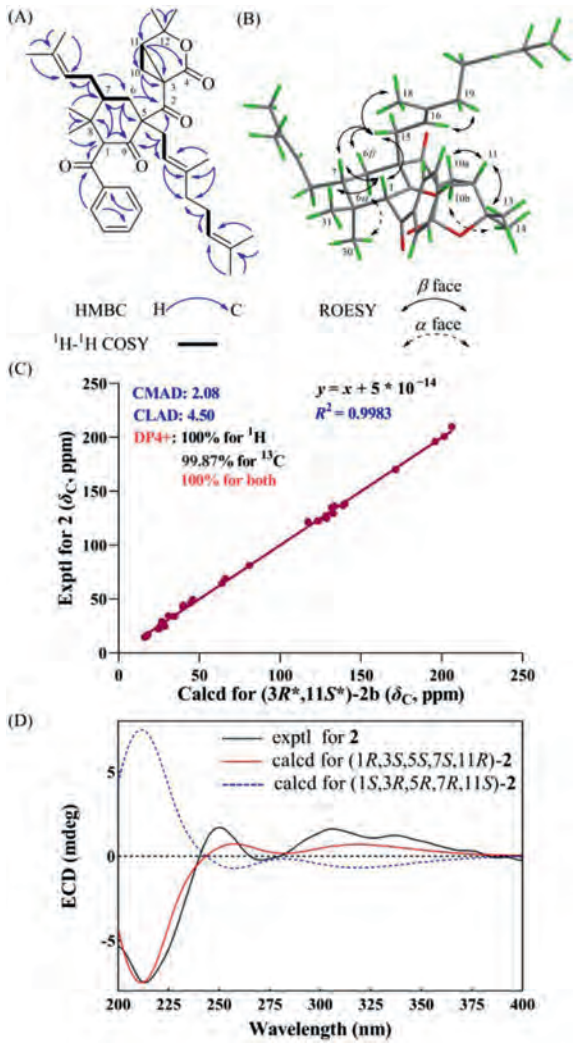

Fig. 4. 2D NMR spectra analysis and assignment of the relative and absolute configurations of **2**. (A) Key HMBC and ^{1}H–^{1}H COSY correlations of **2**. (B) Key ROESY correlations of **2**. (C) NMR calculations with DP4+ analyses for (3R*,11S*)-**2b**. (D) Experimental and calculated ECD spectra of **2**.

to C-19, C-20 and C-22. Furthermore, the correlations from H_2-15 to C-2, C-5, C-6 and C-9, and from H_2-6, H_2-10, and H-11 to C-2 in the HMBC spectrum indicated the locations of the geranyl group and 4,4-dimethyl-3-oxabicyclo[3.1.0]hexan-2-one moiety (Fig. 4A). Thus, the planar structure of **2** was determined.

The ROESY correlations observed from H-1/H-7, H-1/Me-31, H-6α/Me-30, H_2-15/H-1, H_2-15/H-6β, and H_2-15/H-7 implied that H-1, H-7 and the methylene H_2-15 were on the same face with β-orientations, while the benzoyl group, the prenyl group at C-7 and C-2 carbonyl group were on the same face with α-orientations (Fig. 4B). Further, the 16*E* configuration of C-5 geranyl moiety was confirmed by the ROESY correlations occurring between Me-18 and H-15a and between H_2-19 and H-16 (Fig. 4B). The structural inflexibility of the 3-oxabicyclo[3.1.0]hexan moiety in **2** restricted that the relative configurations of the bridgehead C-3 and C-11 should be 3*S**,11*R** or 3*R**,11*S**. This assignment was also confirmed by the cross-peaks of H-11/Me-13, H-11/H-10a, and H-10b/Me-14 in its ROESY spectrum. To further confirm the relative configuration of C-3 and C-11, a quantum chemical prediction of ^{1}H and ^{13}C chemical shifts of two isomers (1*S**,3*S**,5*R**,7*R**,11*R**)-**2a** and (1*S**,3*R**,5*R**,7*R**,11*S**)-**2b** were conducted. The absolute difference between calculated and experimental ^{13}C NMR chemical shifts of (1*S**,3*R**,5*R**,7*R**,11*S**)-**2b** were within 5 ppm, while the calculated ^{13}C NMR chemical shifts of (1*S**,3*S**,5*R**,7*R**,11*R**)-**2a** showed large discrepancies at C-3, C-11, and C-33 (Table S3-4 in Supporting information). Further, applying the DP4+ algorithm to shielding tensors produced 100% confidence that 1*S**,3*R**,5*R**,7*R**,11*S** best fits the experimental data (Fig. 4C and Fig. S1-1B in Supporting information). The absolute configuration of **2** was determined by comparative analysis of computed and experimental ECD spectra, which assigned the 1*R*,3*S*,5*S*,7*S*,11*R* (Fig. 4D) absolute configuration for **2**.

Inspired by the structure of a co-isolated known PPAP (**3**) with a C-5 geranyl-decorated bicyclo[3.3.1]nonane core, a plausible biogenetic pathway (Scheme 1) was proposed, in which compounds **1**–**3** were deemed to be derived from an assumed bicyclo[3.3.1]nonane PPAP precursor (I). Starting from the precursor I, an *O*-cyclization step led to compound **3**. Then, through a pivotal retro-Claisen rearrangement of the enolizable β,β'-triketone motif, the key intermediate II with a typical 1,2-*seco*-bicyclo[3.3.1]nonane-derived core was constructed [17–19]. Further, the chemodivergent radical cascade cyclizations between a β-keto acid group and pendent prenyl or geranyl groups in the structure of II yielded compounds **1** and **2**. The 5-*exo*-*trig* radical cyclization of a functionalized β-keto acid group and geranyl group led to the intermediate III, which would undergo another 5-*exo*-*trig* radical

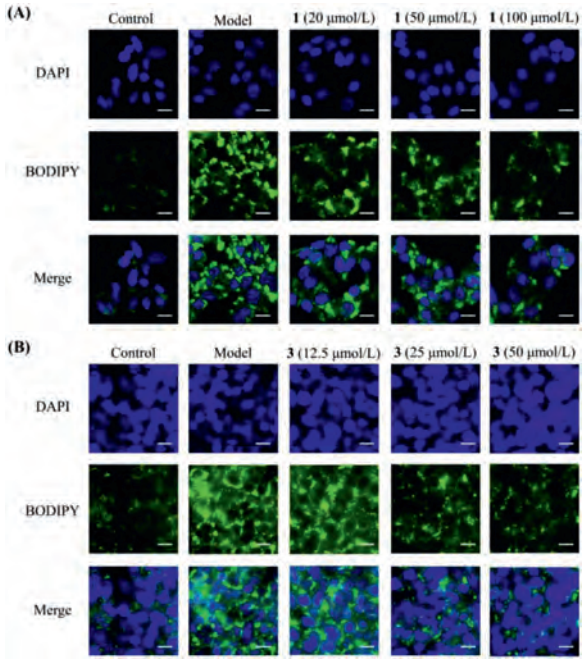

Fig. 5. Lipophilic dye BODIPY 493/503 images of compounds **1** (A) and **3** (B) anti-NASH screening in HepG2 cells. DAPI: 2-(4-Amidinophenyl)-6-indolecarbamidine dihydrochloride; BODIPY: Boron-dipyrromethene, 4,4-difluoro-4-bora-3a,4a-diaza-*s*-indacene. Scale bar: 20 μm.

cyclization to the intermediate IV and then esterification to give compound **1** [20]. Referring to the similar radical cyclization, II could also undergo a 3-*endo*-*trig* radical cyclization of the β-keto acid moiety and $\Delta^{11,12}$ double bond in the pendent prenyl moiety to afford compound **2** [20].

Growing evidences have supported the beneficial role of natural products in treating NASH [21–23]. In the previous reports, many sub-types of PPAPs exhibited significant anti-NASH activity [24,25]. Compound **1** showed no cytotoxicity against HepG2 cell lines up to 200 μmol/L, while compounds **2** and **3** showed no cytotoxicity against HepG2 cell lines up to 50 μmol/L (Fig. S1-4 in Supporting information). The effects of **1**–**3** on cellular lipid levels were explored in a palmitic acid-exposed [26,27] HepG2 cell model using the lipophilic dye BODIPY 493/503 [28]. The images of lipophilic dye BODIPY 493/503 in Fig. 5 showed that **1** and **3** could inhibit lipid accumulation in HepG2 cells. Furthermore, quantitative analysis of intracellular lipid droplets showed that **1** and **3** could decrease the lipid droplets in a dose-dependent manner (Fig. S1-5 in Supporting information). These results indicated that compounds **1** and **3** might be appealing to medicinal chemists for further investigation as a potential protective agent against NASH development.

In summary, 1,2-*seco* and rearranged bicyclo[3.3.1]nonane PPAP possessing an unprecedented spiro[bicyclo[3.3.0]octane-3,1′-cyclohexane]-2,2′–dione core and an unusual 4,4-dimethyl-3-oxabicyclo[3.1.0]hexan-2-one moiety, hyperbenzones A (**1**) and B (**2**), respectively, along with a known biosynthetic congener otogirinin D (**3**) [15], were isolated from *H. beanii*. Biogenetically, the 1,2-*seco* retro-Claisen rearrangement in combination with the following chemodivergent radical cyclizations from a bicyclo[3.3.1]nonane PPAP precursor afforded compounds **1** and **2**. In addition, the bioassay showed that both compounds **1** and **3** could decrease intracellular lipid accumulation in a palmitic acid-induced NASH cell model. This work indicated that the cleavage and further cyclization of the enolizable β,β'-triketone moiety in the bicyclo[3.3.1]nonane core of PPAP could continuously generate significant structural complexity and diversity of PPAPs.

Declaration of competing interest

The authors declare that they have no known competing financial interests or personal relationships that could have appeared to influence the work reported in this paper.

Acknowledgments

This work was supported by the National Natural Science Foundation of China (Nos. 31900287 and 81773886), the 111 Project from Ministry of Education of China and the State Administration of Foreign Export Affairs of China (No. B18056), and Special fund from the Central Committee for guiding local scientific and technological development of Shenzhen (No. 2021Szvup161).

Appendix A. Supplementary data

Supplementary material associated with this article can be found, in the online version, at doi:10.1016/j.cclet.2021.11.011.

References

[1] R. Ciochina, R.B. Grossman, Chem. Rev. 106 (2006) 3963–3986.
[2] X.W. Yang, R.B. Grossman, G. Xu, Chem. Rev. 118 (2018) 3508–3558.
[3] H. Bridi, G.C. Meirelles, G.L. von Poser, Phytochemistry 155 (2018) 203–232.
[4] E. Iglesias, Curr. Org. Chem. 8 (2004) 1–24.
[5] N. Zhang, Z.Y. Shi, Y. Guo, et al., Org. Chem. Front. 6 (2019) 1491–1502.
[6] Y. Guo, Q.Y. Tong, N. Zhang, et al., Org. Chem. Front. 6 (2019) 817–824.
[7] R.D. Liu, Y.L. Su, J.B. Yang, A.G. Wang, Phytochemistry 142 (2017) 38–50.
[8] S.S. Xie, C.X. Qi, Y.L. Duan, Org. Chem. Front. 7 (2020) 1349–1357.
[9] Y.L. Hu, K. Hu, L.M. Kong, et al., Org. Lett. 21 (2019) 1007–1010.
[10] H.Y. Lou, Y.N. Li, P. Yi, et al., Org. Lett. 22 (2020) 6903–6906.
[11] J.J. Zhang, X.W. Yang, X. Liu, et al., J. Nat. Prod. 78 (2015) 3075–3079.
[12] Z.Z. Zhang, Y.R. Zeng, Y.N. Li, et al., Org. Org. Biomol. Chem. 19 (2021) 216–219.
[13] W.J. Xu, P.F. Tang, W.J. Lu, et al., Org. Lett. 21 (2019) 8558–8562.
[14] W.X. Li, W.J. Xu, J. Luo, L. Yang, L.Y. Kong, Chin. J. Nat. Med. 19 (2021) 385–390.
[15] Y. Ishida, O. Shirota, S. Sekita, et al., Chem. Pharm. Bull. 58 (2010) 336–343.
[16] X.W. Yang, J. Yang, Y. Liao, et al., Tetrahedron Lett. 56 (2015) 5537–5540.
[17] G. Grogan, G.A. Roberts, D. Bougioukou, N.J. Turner, S.L. Flitsch, J. Biol. Chem. 276 (2001) 12565–12572.
[18] Y.G. Yatluk, S.V. Chernyak, A.L. Suvorov, E.A. Khrustaleva, V.I. Abramova, Russ. J. Gen. Chem. 7 (2001) 965–967.
[19] M. Jukic, D. Sterk, Z. Casar, Curr. Org. Synth. 9 (2012) 488–512.
[20] J.H. George, M.D. Hesse, J.E. Baldwin, R.M. Adlington, Org. Lett. 12 (2010) 3532–3535.
[21] Y. Takahashi, K. Sugimoto, H. Inui, T. Fukusato, World J. Gastroenterol. 21 (2015) 3777–3785.
[22] T. Yan, N. Yan, P. Wang, et al., Acta Pharm. Sin. B 10 (2020) 3–18.
[23] Y.R. Leng, M.H. Zhang, J.G. Luo, H. Zhang, Chin. J. Nat. Med. 19 (2021) 12–27.
[24] W.J. Lu, W.J. Xu, M.H. Zhang, et al., J. Nat. Prod. 84 (2021) 1135–1148.
[25] X. Zhou, W.J. Xu, Y.R. Li, et al., J. Agric. Food Chem. 69 (2021) 646–654.
[26] S. Joshi-Barve, S.S. Barve, K. Amancherla, et al., Hepatology 46 (2007) 823–830.
[27] H. Utsunomiya, Y. Yamamoto, E. Takeshita, et al., J. Gastroenterol. 52 (2017) 940–954.
[28] L. Zhao, C. Zhang, X. Luo, et al., J. Hepatol. 69 (2018) 705–717.